

Dynamic Behavior of Gas Permeation in Solid Polymer Electrolyte Membranes*

by Tohru KANNO**, Shinji FUJITA***, Yoshikazu SASAKI****
and Masayoshi KOBAYASHI**

(Received October 13, 1988)

Abstract

The permeabilities of ethylene, propylene and carbon dioxide through various solid polymer electrolyte (SPE) membranes such as Nafion 417 (N-417), Asahikasei K-101 and A-201 and metal ion modified membranes have been compared at temperature ranges 0~80°C, using a flow-type diffusion cell newly developed for gas permeation under atmospheric pressure. K-101 and A-201 give no reproducibility of the permeability because of the cracks irreversibly formed on the membranes during the diffusion of gases, whereas N-417 gives a good reproducibility despite a small amount of permeability. On the silver-supported membrane, the permeabilities of C₂H₄ and C₃H₆ are clearly enhanced 2~3 times even though CO₂ is reduced to one third, and this is suggested by the formation of silver-olefin complexes which work as a pump to carry olefin gas. On the nickel-supported membranes, permeability is always reduced because the ion channel of the membrane for gas diffusion is diminished by the metal ions.

1. Introduction

Solid Polymer Electrolyte (SPE) membranes have been extensively studied for use as one of the new multi-functional materials for gas and liquid separation or condensation¹⁻⁴, fuel cells⁵, water electrolysis⁶, brine electrolysis⁷, and censor and electro-organic synthesis⁸⁻¹⁰. Recently, Nafion-supported metals have been used for heterogenized homogeneous catalytic processes^{11,12}. For gas separation, considerable efforts have been devoted to developing artificial organs such as artificial lungs and extracorporeal membrane oxygenators for patients suffering from respiratory illnesses. Monsanto Co. developed a membrane to recover hydrogen from a product mixture of an ammonia synthesis process. A membrane to concentrate oxygen in air is extremely useful to save energy for the liquid nitrogen and oxygen industries, and for combustion furnaces. The separation of olefins might be useful for the C₁-Chemical Industry to separate gas mixtures which are formed.

The object of the research reported in this paper is to develop a new diffusion cell measuring the permeability of gases under a steady state flow system.

* The paper was presented at the Hokkaido regional meeting of the Chemical Society of Japan in the winter period of 1988 and the national meeting of the Chemical Engineering Society of Japan in 1988.

** Department of Industrial Chemistry.

*** Department of Chemical Environmental Engineering.

**** Paroma Co.

Another object is to clarify the permeability behavior of C_2H_4 , C_3H_6 and CO_2 using commercial SPE membranes and metal ion supported membranes.

2. Experimental Section

(1) Membranes

Three commercial membranes (Asahikasei K-101 and A201 and Nafion 417) were used as functional membrane for gas separation. Although the detailed structures of K-101 (dark orange color, cation-exchanged type, and 200 μm thick) and A-201 (white, anion-exchanged type, and 250 μm thick) were not reported, cation and anion might be connected with the end groups of the molecules constituting the membranes respectively.

Nafion 417 is a cation exchange membrane and has the exchange capacity of 1100 eq/g and a thickness of 0.04318 cm. Fig. 1 illustrates a schematic representing the cluster morphology of the membrane¹³⁾. The general form of the membrane is expressed as follows.

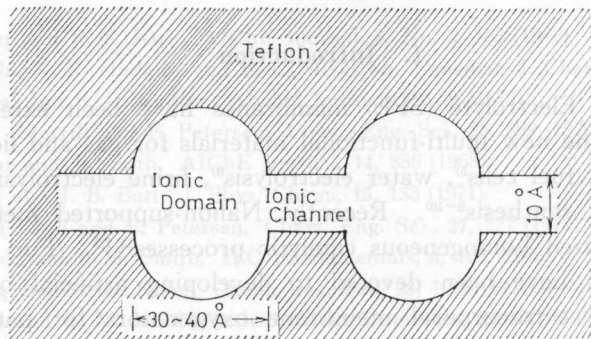
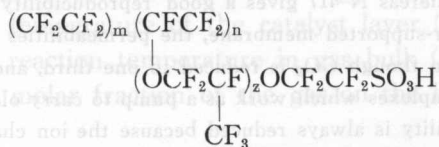


Fig. 1. Schematic representation of the cluster morphology of SPE membrane.

(2) Preparation of the Metal-Supported Membranes

Silver and nickel metal ions were supported in/on the membranes by the following two methods.

Soaking Method (Ag):

Pieces of the membranes at a constant weight of 1.75 g ($10 \times 2.5 \times 0.04318$ cm³) were immersed in 0.1 N- $AgNO_3$ solution at room temperature for a week. The amount of silver supported was analysed to be 6.84 (mg-Ag/cm²-membrane) by the titration method using KSCN solution.

Takenaka-Torikai Method (Ag and Ni):

Ag:

This method was developed first by H. Takenaka and E. Torikai¹⁰. The membranes were immersed in water at 80°C for 2 hrs. For supporting the metals, a box (made of acrylate resin) which was divided into two compartments (each of which was $1.0 \times 0.9 \times 9.0 \text{ cm}^3$) by the membrane was prepared. Two different solutions were separately poured into the two compartments: (1) 0.1N-NaBH₄+0.1N-NaOH and (2) 0.1N-AgNO₃ solution. The reaction between the two solutions was allowed to continue in/on the membrane which was sandwiched between the two compartments for 24 hrs. The modified membrane thus obtained was washed carefully with redistilled water and dried at room temperature for 24 hrs. The amount of supported silver was analysed to be 6.7 (mg-Ag/cm²-membrane) by the titration with 0.1N-KSCN solution using an iron alum as an indicator.

Ni:

The experimental procedure was the same one as for Ag, except the solutions in the two compartments were (1) 1N-Ni(NO₃)₂ and (2) 0.1N-NaBH₄+0.1N-NaOH. The nickel supported membrane became green after the reaction for 24 hrs. The amount of supported nickel metal which was analysed by the atomic absorption spectroscopy was 7.89 (mg-Ni/cm²-membrane).

(3) Diffusion Cell

Fig. 2 illustrates the schematic drawings of the diffusion cell used in this study. The cell consisted of two flat plates (stainless steel, $8 \times 0.95 \times 0.105 \text{ cm}^3$) in each of which a groove was prepared for the gas flow, and the membrane was sandwiched between the two plates. The groove of the two plates was divided by the membrane. The gases in both grooves partly permeated between the two plates through the membrane, with a counter current. The permeation through the membrane from one side to the other side was visualized in the figure. The diffusion area was 7.6 cm² and the groove volume was 0.798 cm³.

The diffusion cell was put into a water bath the temperature of which was well controlled within the accuracy of $\pm 1^\circ\text{C}$ at the given temperature.

(4) Procedure and Measurements of Diffusion

Fig. 3 illustrates the flow diagram of the experimental system. Three flow-

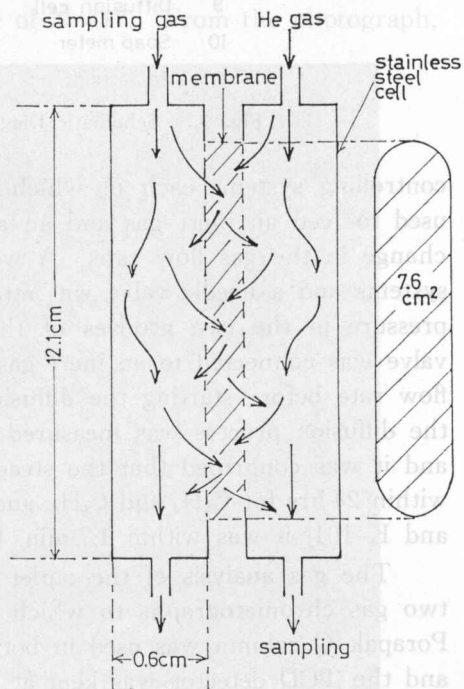


Fig. 2. The diffusion cell used in this study.

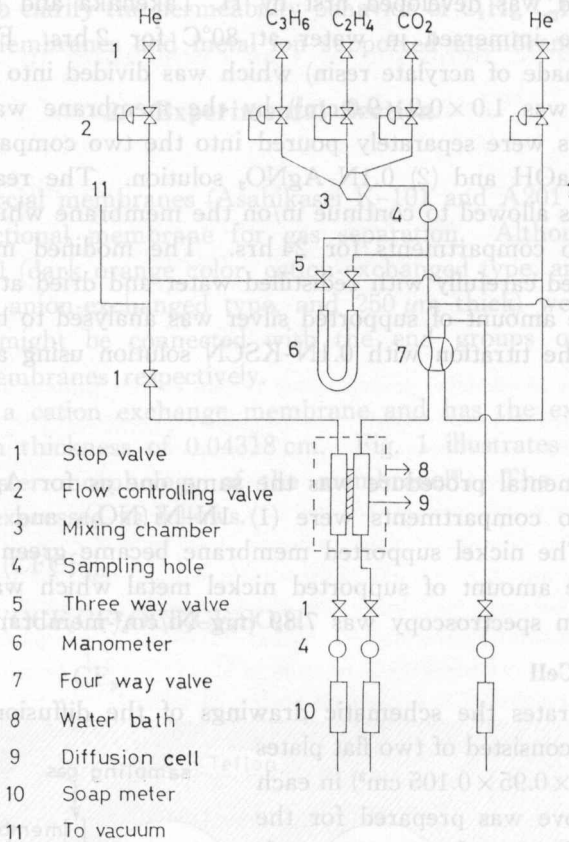


Fig. 3. Schematic Diagram of the experimental equipment.

controlling systems each of which could prepare a different gas mixture were used to feed an inert gas and an adsorptive gas into the diffusion cell with no change in the gas flow rate. A water manometer was connected to the three systems and a needle valve was attached to the outlet of the cell to ensure the pressure in the two grooves of the diffusion cell was equalized. A four-port valve was connected to an inert gas stream groove (He) to measure the absolute flow rate before starting the diffusion measurement. The transient response of the diffusion process was measured by using the transient response method¹⁵⁻¹⁷, and it was confirmed that the steady state of diffusion for N-417 was obtained within 24 hrs for C_2H_4 and C_3H_6 , and within 4 hrs for CO_2 . In the case of A-201 and K-101, it was within 1.7 min. for CO_2 , C_2H_4 and C_3H_6 .

The gas analysis of the outlet streams of the two sides was conducted by two gas chromatographs to which TCD and FID detectors were attached. A Porapak Q column was used in both cases to separate CO_2 , C_2H_4 , C_3H_6 and He, and the TCD detector was kept at $70^\circ C$ with a 2 m column length and the FID detector was kept at $200^\circ C$ with a 1 m column length.

(5) Gases

The gases used in this study were commercially prepared with no further purification supplied from Hokusan (CO_2 and He) and Shinnihon Seitetsu Chemicals (C_2H_4 and C_3H_6). The purity was CO_2 (99.5%), He (99.995%), C_2H_4 (99.0%) and C_3H_6 (99.5%).

3. Results and Discussion

3-1. Characterization of the Membranes

(1) Scanning Electron Microscopy (SEM) and Electron Diffraction Analysis (EDA) Photographs

Figs. 4 and 5 illustrate SEM photographs of N-417 and the metal-supported membranes respectively. One can see that the surfaces of these membranes were rather rough and heterogeneous.

For the metal-supported membranes, the metals were always localized to form many islands in different sizes on the surfaces. From the photos, one may observe a difficulty in getting a homogeneous dispersion of metals on the surface and inside of the membranes in the present procedure.

Fig. 6 illustrates the EDA photographs of the metal-supported membranes. The results clearly show that the islands formed on the surface are composed of Ag. In these techniques, it is difficult to evaluate separately the amounts of metals supported between the surface and inside of the membrane. Fig. 7 shows a SEM photograph of the cross-sectional view of N-417. From the photograph,

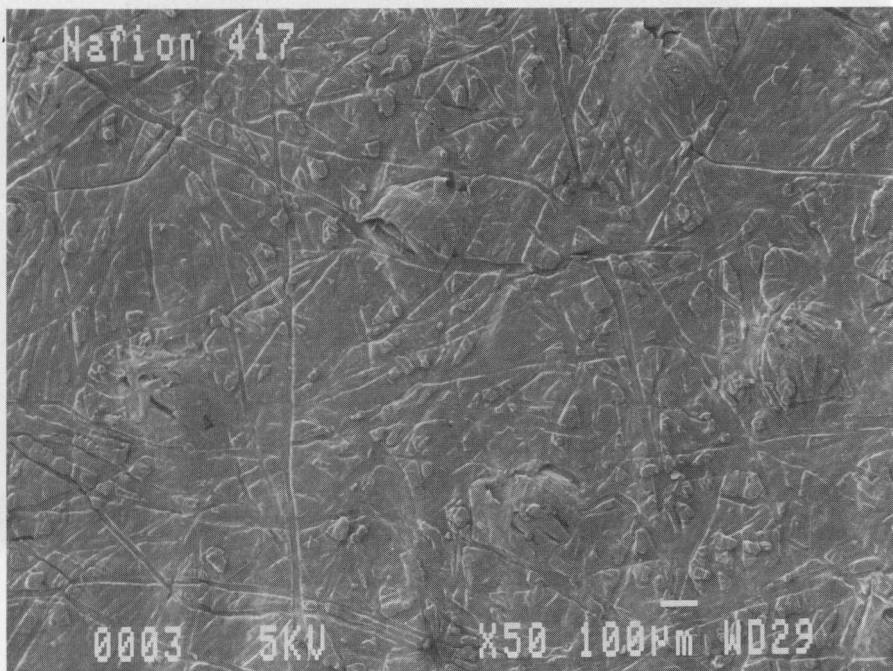
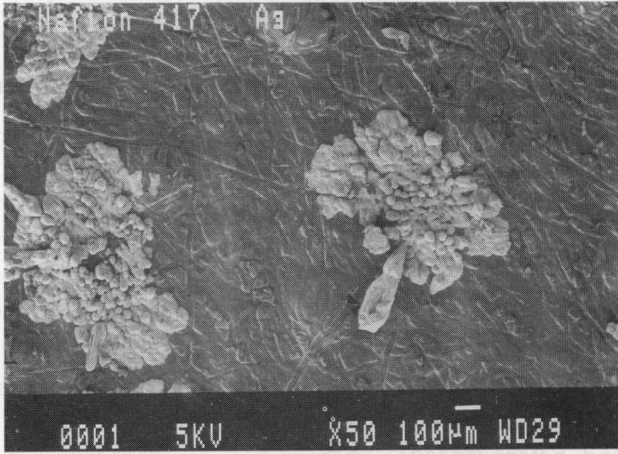
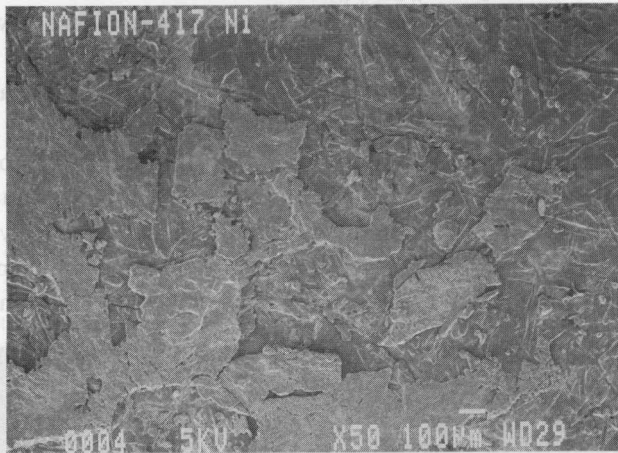


Fig. 4. SEM photograph of N-417.

(a) N-417



(b) Ni-N-417



(c) Ag-K-101

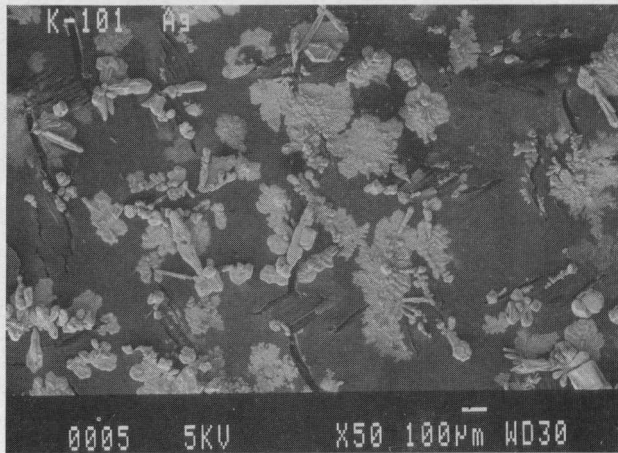


Fig. 5. SEM photographs of Ag and Ni supported N-417 and K-101.

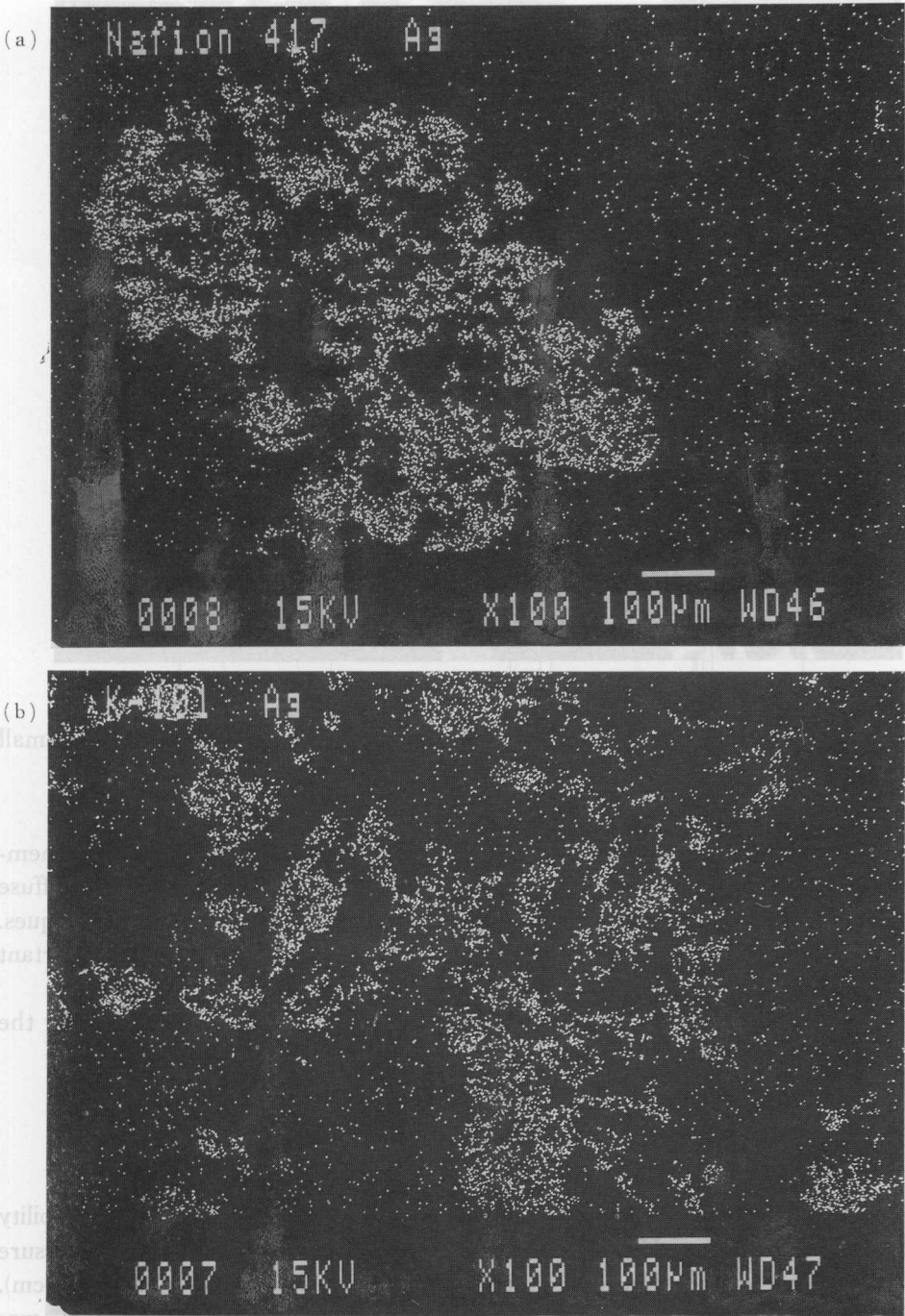


Fig. 6. EDA photographs of Ag supported (a) N-417 and (b) K-101.

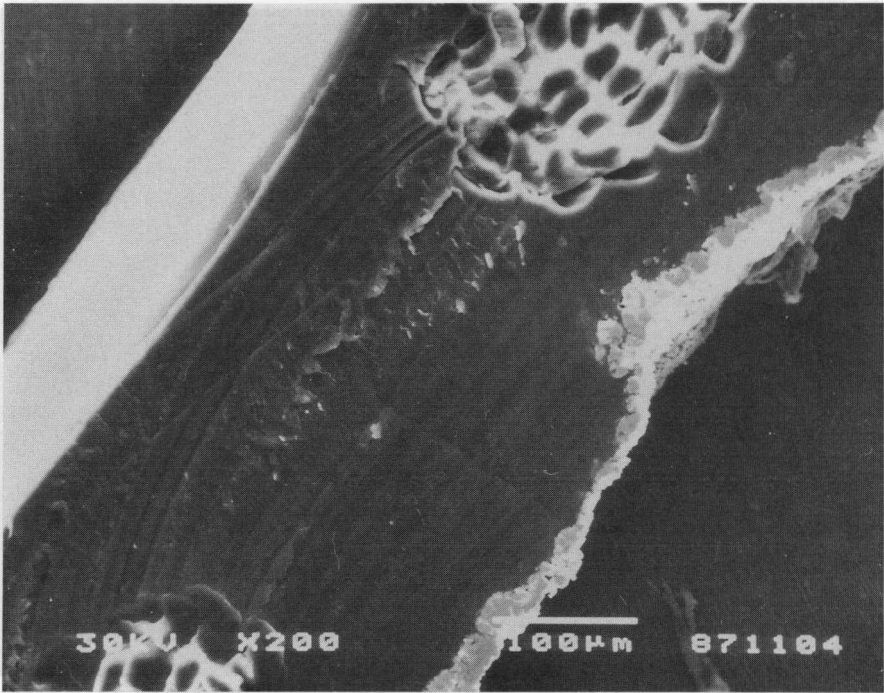


Fig. 7. SEM photograph of the cross sectional view of Ag supported N-417.

one can not see any information on the metal particles because of too small amounts to detect.

(2) Infrared Spectroscopy

Figs. 8 a and b show the IR spectra of the SPE and Ag-supported membranes. The IR spectra were obtained by two different procedures: the diffuse reflectance infrared fourier transform and the ordinary IR transmission techniques. At the present time, it is not easy to assign all the spectra. All the important absorption bands are presented in Table 1 roughly assigned.

No appreciable change in the absorption bands is recognized between the membrane and Ag-supported ones.

3-2. Comparison of the Gas Permeabilities in the Membranes

The permeation coefficient of gases was calculated by Equation (1)

$$Q = PS/l \quad (1)$$

where Q is the amount of permeated gas per sec ($\text{cm}^3(\text{STP})/\text{sec}$), P is permeability ($\text{cm}^3(\text{STP}) \cdot \text{cm}/\text{cm}^2 \cdot \text{sec} \cdot \text{cmHg}$), S is diffusion area (cm^2), p_1 and p_2 are partial pressure of the two rooms in the diffusion cell (cmHg) and l is thickness of membrane (cm).

The gas permeability (P_{g_0}) of the membranes for CO_2 , C_2H_4 and C_3H_6 was measured at various temperatures and the results are presented in Figs. 9, 10 and 11. The permeabilities of various membranes are represented in Table 2. Our interest is focused on the various differences of P_{g_0} between K-101, A-201 and N-417. Comparing the values of P_{g_0} to other SPE membranes, N-417 is

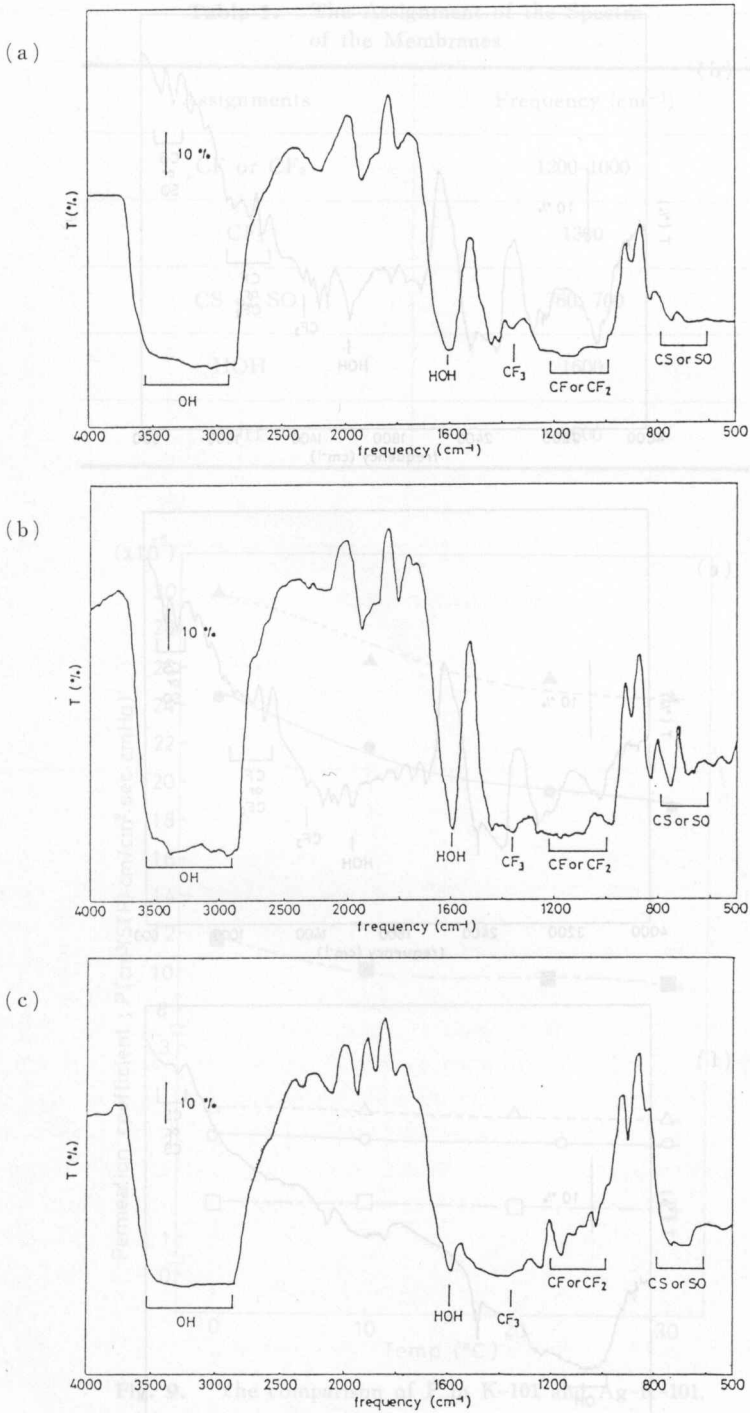


Fig. 8 a. Comparison of the IR spectra of (a) K-101, (b) Ag-K-101 and (c) A-201 by the transmission technique.

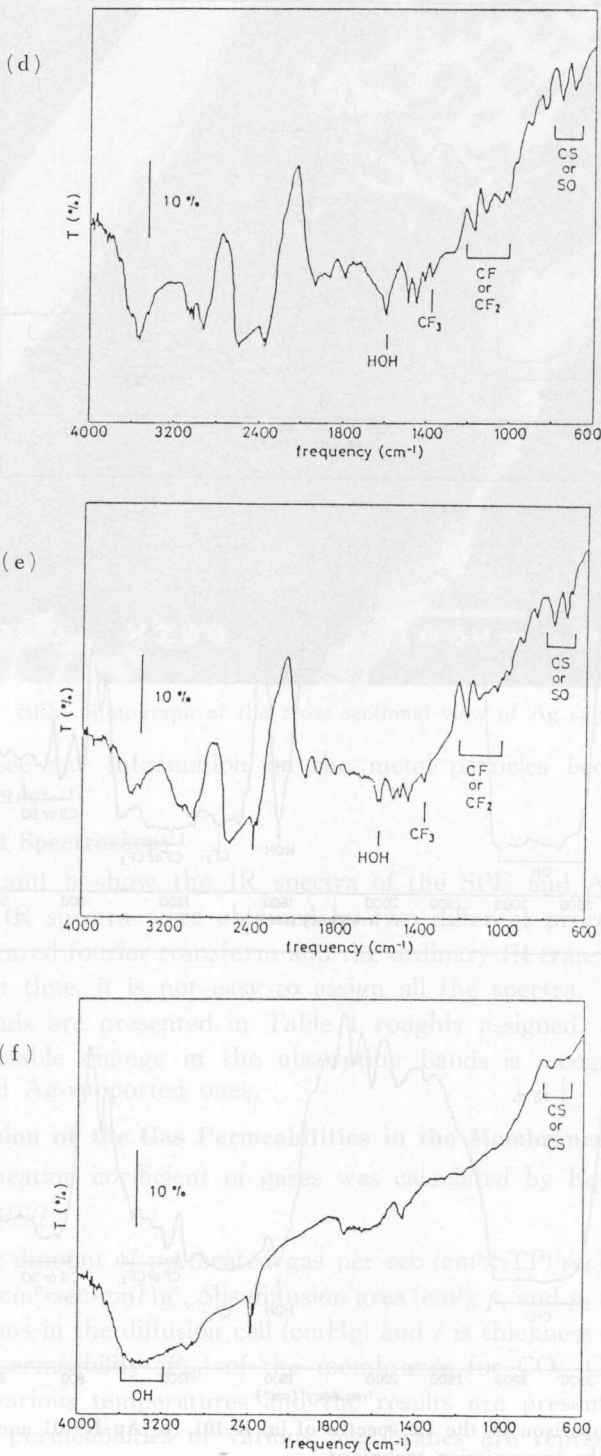


Fig. 8b. Comparison of the IR spectra of the DRIFTS of (d) K-101, (e) A-201 and (f) N-417.

Table 1. The Assignment of the Spectra of the Membranes

Assignments	Frequency (cm ⁻¹)
CF or CF ₂	1200-1000
CF ₃	1360
CS or SO	760, 700
HOH	1600
OH	3600

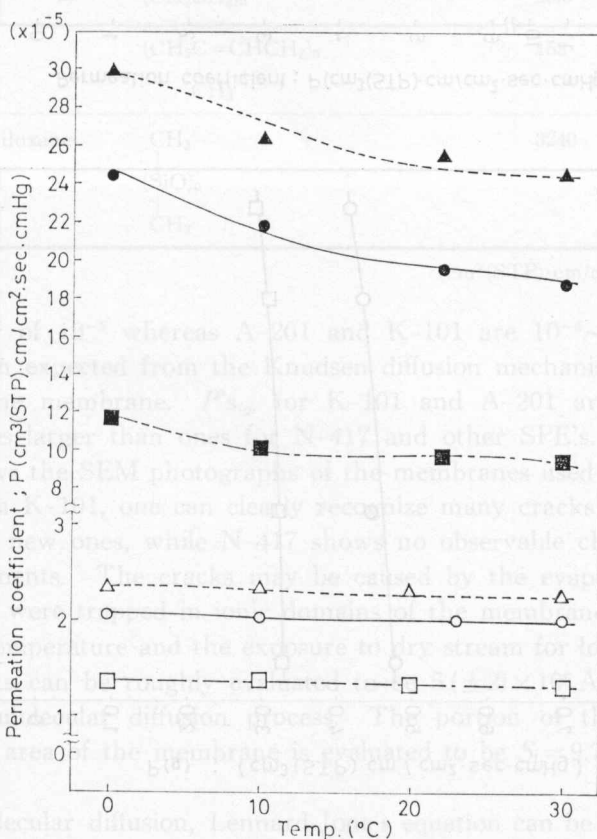


Fig. 9. The comparison of P in K-101 and Ag-K-101.

○, ●; CO₂ △, ▲; C₂H₄ □, ■; C₃H₆
 open; K-101 occupied; Ag-K-101

D_{AB} is diffusion coefficient of A into B-gas (cm²/sec), M_A and M_B are the mole

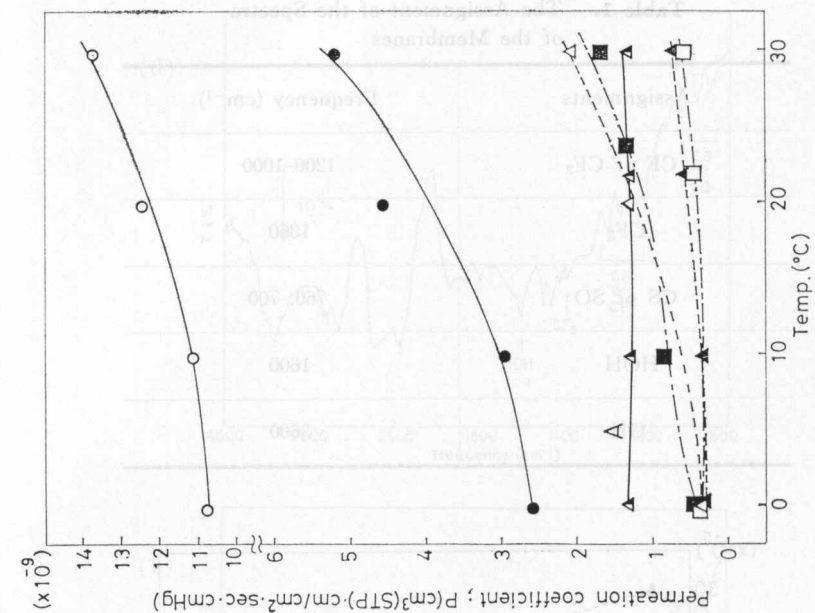


Fig. 11. The comparison of P in Nafion 417 and Ag-Nafion 417.
 O, ●; CO₂ △, ▲; C₂H₄ □, ■; C₃H₆
 open; Nafion occupied; Ag-Nafion

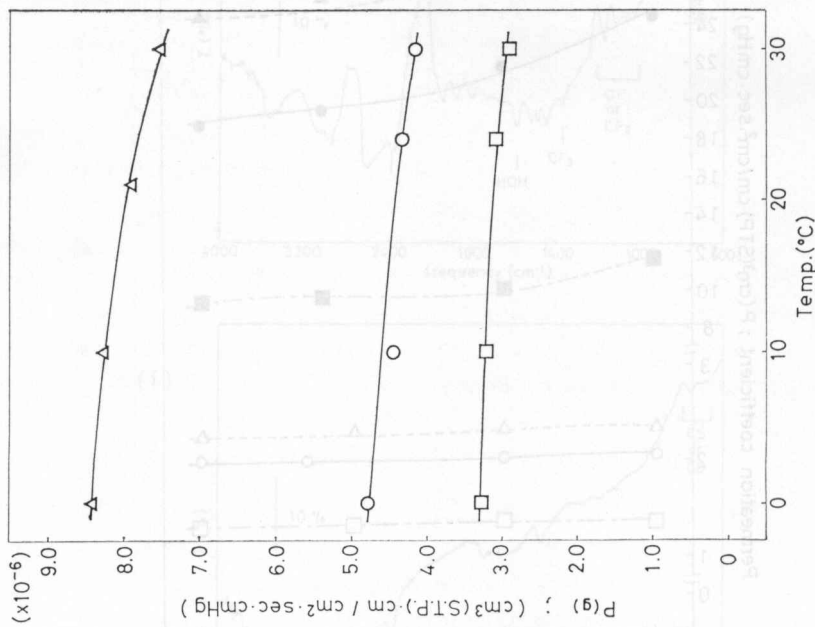


Fig. 10. P(g) as a function of Temp. for A-201.
 △; C₂H₄ O; CO₂ □; C₃H₆

Table 2. Comparison of the Permeability of CO₂ in the various membranes at 25°C

	chemical structure	permeability ($\times 10^{-10}$)
Nafion-417	$ \begin{array}{c} (\text{CF}_2\text{CF}_2)_m(\text{CF}_2\text{CF}_2)_n \\ \\ (\text{OCF}_2\text{CF}_2)_x\text{OCF}_2\text{CF}_2\text{SO}_3\text{H} \\ \\ \text{CF}_3 \end{array} $	129
A-201		42400
K-101		220000
polyacrylonitrile	$ \begin{array}{c} (\text{CH}_2\text{CH})_n \\ \\ \text{CN} \end{array} $	0.0018
polytetrafluoro-ethylene	$ (\text{CF}_2\text{CF}_2)_n $	12.7
polyethylene	$ (\text{CH}_2\text{CH}_2)_n $	28.0
natural rubber	$ \begin{array}{c} (\text{CH}_2\text{C}=\text{CHCH}_2)_n \\ \\ \text{CH}_3 \end{array} $	153
polydimethyl-siloxane	$ \begin{array}{c} \text{CH}_3 \\ \\ (\text{SiO})_n \\ \\ \text{CH}_3 \end{array} $	3240

(cm³(STP)·cm/cm²·sec·cmHg)

within the order of 10^{-8} whereas A-201 and K-101 are $10^{-6} \sim 10^{-5}$ which are much larger than expected from the Knudsen diffusion mechanism based on the micro pore of the membrane. $P_{s(\varphi)}$ for K-101 and A-201 are thereby about 10^3 and 10^2 times larger than ones for N-417 and other SPE's.

Fig. 12 shows the SEM photographs of the membranes used for the diffusion experiments. On K-101, one can clearly recognize many cracks which were not observed on the new ones, while N-417 shows no observable changes before or after the experiments. The cracks may be caused by the evaporation of water molecules which were trapped in ionic domains of the membrane, resulting from the increase of temperature and the exposure to dry stream for long period. The size of the cracks can be roughly evaluated to be $5(\pm 2) \times 10^6 \text{ \AA}$ where gas permeates by the molecular diffusion process. The portion of the cracked area against the total area of the membrane is evaluated to be $S_1 = 9.7 \times 10^{-3} (\text{cm}^2/\text{cm}^2\text{-membrane})$.

For the molecular diffusion, Lennard-Jone's equation can be used to estimate the diffusion coefficient^{18,19}.

$$D_{AB} = \frac{0.001858T^{3/2}[(M_1 + M_2)/M_1 M_2]^{1/2}}{\pi \sigma_{AB}^2 \Omega_D} \quad (2)$$

D_{AB} is diffusion coefficient of A into B-gas (cm²/sec), M_A and M_B are the mole-

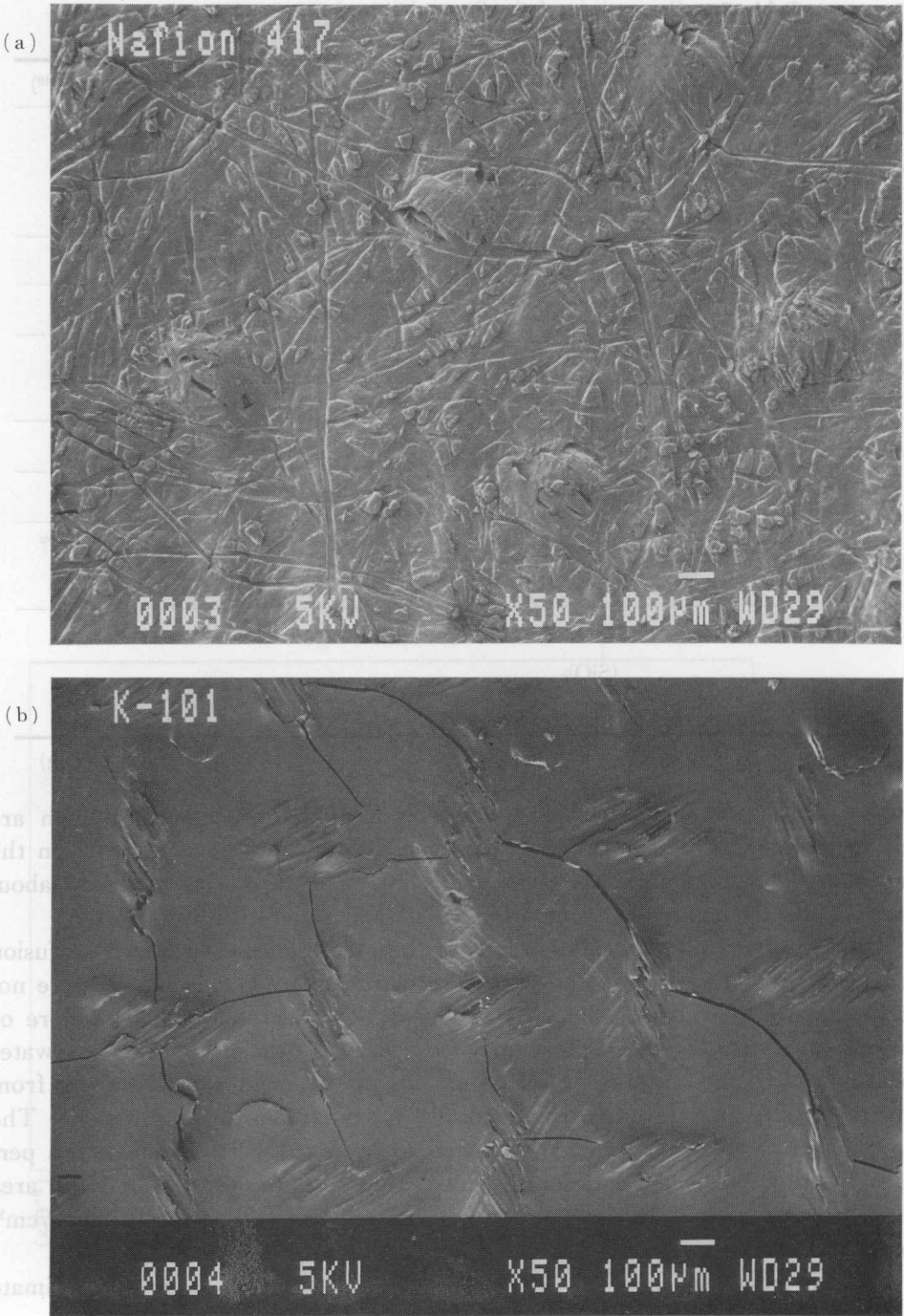


Fig. 12. SEM photographs of (a) N-417 and (b) K-101 membranes used for diffusion experiments.

cular weights of *A* and *B*-gas (g/mole), *T* is temperature (296°K), π is total pressure (atm), σ_{AB} is the force constant (Å), and Ω_D is the "collision integral" which is a function of $kT/\varepsilon_{AB}(-)$, and ε_{AB} is the Lennard-Jones potential (J).

In the He-CO₂ diffusion system, using $M_A=4$, $M_B=44$, $\sigma_A=2.576$ (Å), $\sigma_B=3.996$ (Å), $\sigma_{AB}=1/2(\sigma_A+\sigma_B)=3.286$ (Å), $\varepsilon_A/k=10.22$ (°K), $\varepsilon_B/k=190$ (°K), $\varepsilon_A=1.410 \times 10^{-22}$, $\varepsilon_B=2.622 \times 10^{-21}$ and $\varepsilon_{AB}=\sqrt{\varepsilon_A\varepsilon_B}=6.080 \times 10^{-22}$, kT/ε_{AB} and Ω_D can be calculated to be 6.718 and 0.8060 respectively. D_{AB} is thus calculated to be 0.57 (cm²/sec). Using Fick's equation, the diffusion area (S_2) can be evaluated by Eq. (3).

$$S_2 = \left(\frac{dN_A}{dt} \right) \frac{1}{D_{AB}} \frac{\Delta L}{\Delta C_A} \quad (3)$$

where N_A is moles of diffusion gas *A* (mole), *t* is time (min), ΔL is thickness of the sample (cm), ΔC_A is the concentration difference between the two compartments* (mole/cm³). Using the experimental conditions $dN/dt=6.866 \times 10^{-6}$ (mol/sec), $\Delta L=0.02$ cm and $\Delta C_A=1.08 \times 10^{-5}$ (mol/cm³), S_2 is evaluated to be 2.2×10^{-2} (cm²/cm²-membrane). Comparing S_2 to S_1 , the two values roughly agree in the order with no serious error. This agreement strongly suggests that the diffusion in K-101 and A-201 membranes is controlled by the molecular diffusion because of the cracks ($5(\pm 2) \times 10^6$ Å) evolved during the diffusion measurements.

$P'_{s(q)}$ of K-101 and A-201 (see Fig. 10) are decreased with the temperature which is an inverse tendency compared to N-417. This inverse tendency may result from the reduction of the crack size of the membranes due to the thermal expansion of the membrane body with increasing temperature. On $P_{(q)}$ for N-417, the value is ordered as CO₂ ($\bar{d}=4.60$ Å) > C₂H₄ ($\bar{d}=5.05$ Å) > C₃H₆ ($\bar{d}=5.53$ Å) depending on their molecular sizes, suggesting the Knudsen diffusion mechanism is taking place through the ionic channels and domains in the membrane²⁰.

3-3. Permeabilities in the Metal-Supported Membranes

Fig. 9 illustrates $P'_{s(q)}$ of CO₂, C₂H₄ and C₃H₆ as a function of temperature for silver-supported K-101 (designate Ag-K-101). All the values of $P_{(q)}$ are 8~13 times larger than those for the membrane only. This enhancement can reasonably be considered as the physical expansion of the crack size because of the supported silver.

Fig. 11 illustrates $P'_{s(q)}$ of CO₂, C₂H₄, and C₃H₆ for N-417 and silver-supported

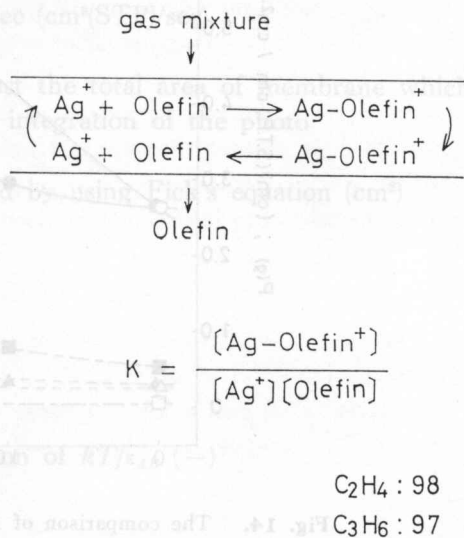


Fig. 13. Schematic explanation of the pumping effect of Ag-olefin complex.

N-417 (designate Ag-N-417) as a function of temperature. $P_{(g)}$ of CO_2 is reduced to about one fifth whereas C_3H_6 is rather enhanced 1.3~3.0 times compared to N-417. One can presume the pumping effect of olefin-silver complexes which are formed in the membrane as shown schematically in Fig. 13⁹.

The reduction of $P_{(g)}$ for CO_2 on Ag-N-417 (see Fig. 11) may result from the decrease of diffusion area due to the silver deposited in the pores of membrane. Based on this reduction, one may presume the physical reduction of the diffusion area for C_2H_4 to be about one fifth if the arithmetic calculation is allowed. The values of $P_{(g)}$ obtained experimentally, however, are about 10%~250% higher than the expected ones which are calculated from the reducing percentage of $P_{(g)}$ obtained for CO_2 . The $P_{(g)}$ calculated thus is presented in Fig. 11 by curve A which is clearly higher than the unsupported membrane. From these calculation, one can recognize the enhancement of the supported silver ion in the membrane due to the formation of the Ag-olefin complex which works as a carrier to transfer the olefin gases from one side to the other.

Fig. 14 shows the comparison of $P_{(g)}$ for Ni to Ag-supported N-417. The Ni-supported membrane is always reduced rather than the Ag supported one.

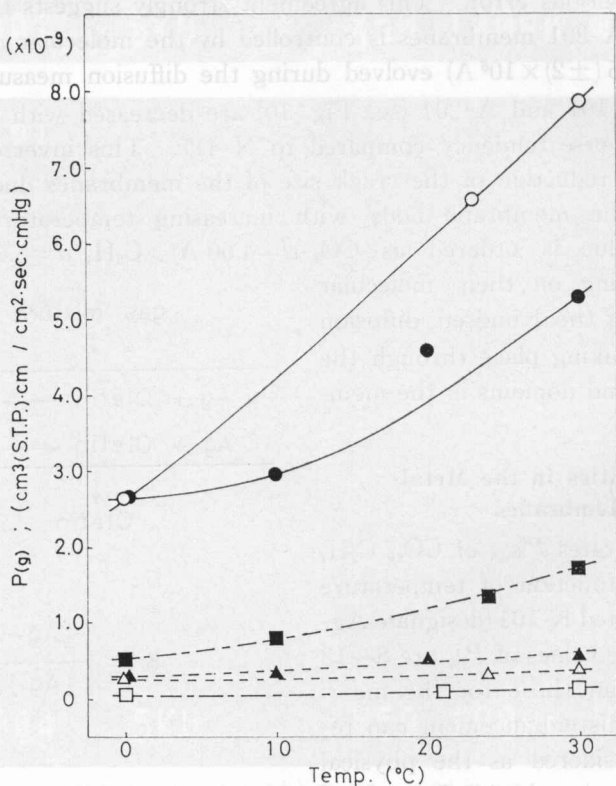


Fig. 14. The comparison of $P_{(g)}$ of Ni and Ag supported N-417 as a function of Temperature.

○, ●; CO_2 △, ▲; C_2H_4 □, ■; C_3H_6
open; Ni-N-417 occupied; Ag-N-417

This clearly indicates that the permeability of the metal-supported membrane is usually reduced if there is no pumping effect of the supported metals, which is caused by the reduction of the diffusion area due to metal ions.

4. Conclusions

Three different commercially prepared SPE membranes (A-201, K-101 and N-417) were used to evaluate their function as gas separation membranes. Reproducible results with N-417 were obtained, and those with the silver-ion supported membrane showed a great enhancement of the permeability for C_2H_4 and C_3H_6 . The permeation mechanism is presumed to be mainly three transport processes: (1) pore diffusion which is the Knudsen flow, (2) the pumping effect due to Ag-olefin complex formed in the membrane and (3) dissolving into the membrane body.

5. Nomenclatures

- ΔC_A : concentration difference between the two compartments in the diffusion cell (mol/cm^3)
- D_{AB} : diffusion coefficient of A into B -gas (cm^2/sec)
- k : Boltzmann constant ($1.38 \times 10^{-23} \text{ J} \cdot \text{K}^{-1}$)
- l : thickness of membrane (cm)
- lL : thickness of sample (cm)
- M_A, M_B : molecular weight of A and B (g/mol)
- N_A : moles of diffusion gas A (moles)
- P : permeation coefficient ($\text{cm}^3(\text{STP}) \cdot \text{cm}/\text{cm}^2 \cdot \text{sec} \cdot \text{cmHg}$)
- p_1, p_2 : partial pressure of the two compartments in the diffusion cell (cmHg)
- Q : amount of permeated gas per sec ($\text{cm}^3(\text{STP})/\text{sec}$)
- S : diffusion area (cm^2)
- S_1 : portion of the crack area against the total area of membrane which is evaluated from the graphical integration of the photo ($\text{cm}^2/\text{cm}^2\text{-membrane}$)
- S_2 : diffusion area which is evaluated by using Fick's equation (cm^2)
- T : temperature ($^\circ\text{K}$)
- t : time (min)

Greek Symbols

- ε : Lennard-Jones potential (J)
- π : total pressure (atm)
- σ_{AB} : force constant (\AA)
- Ω_D : the "collision integral", a function of kT/ε_{AB} ($-$)

* Part of this reports was presented at the JCI conference (June 1986).

** Dept. of Developmental Eng., Faculty of Eng., Khamsi Inst. of Tech.

*** Dept. of Civil Eng., Faculty of Eng., Khamsi Inst. of Tech.

††† Dept. of Civil Eng., Faculty of Eng., Hokkaido Univ.

‡‡†† Taihei Corporation.

6. References

- 1) S. L. Matson, C. S. Herrick, W. J. Ward, *Ind. Eng. Chem. Process Des. Dev.*, **16**, 370 (1977).
- 2) D. L. Ellig, J. B. Althous, F. P. McCandless, *J. Meubr. Sci.*, **6**, 259 (1980).
- 3) D. L. Kuehne, S. K. Friedlauder, *Ind. Eng. Chem. Process Des. Dev.*, **19**, 609, 616 (1980).
- 4) R. D. Hugles, J. A. Mahoney, E. F. Steigelmann, Amoco Research Center (1981)
- 5) Z. Ogumi, Z. Takehara and S. Yoshizawa, *J. Electrochim. Sci., Electrochem. Sci. Tech.*, **131**, No. 4, 769 (1984).
- 6) P. W. T. Lu and S. Srinivasan, *J. Appl. Electrochim.*, **9**, 269 (1979).
- 7) A. P. Laconti, Japan Tokkyo Kokai, 54-112398 (1979).
- 8) Z. Ogumi, K. Nishio and S. Yoshizawa, *Denki Kagaku*, **49**, 212 (1981).
- 9) Z. Ogumi, K. Nishio and S. Yoshizawa, *Electrochim. Acta*, **26**, 1779 (1981).
- 10) Z. Ogumi, H. Yamashita, K. Nishio and S. Yoshizawa, *Electrochim. Acta*, **28**, 1687 (1983).
- 11) V. D. Mattera, Jr., D. M. Barnes, S. N. Chaudhuri, W. M. Risen, Jr., and R. D. Gonzalez, *J. Phys. Chem.*, **90**, 4819 (1986).
- 12) Y. Chauvin, D. Commerreuc and F. Dawans, *Prog. Polym. Sci.*, **5**, 95 (1977).
- 13) W. Y. Hsu and T. D. Gierke, *Macromolecules*, **15**, 101 (1982).
- 14) H. Takenaka and E. Torikai, Kokai Tokkyo Koho (Japan Patent) **55**, 38934 (1980).
- 15) H. Kobayashi and M. Kobayashi, *Catal. Reviews, Sci. Eng.*, **35**, 74 (1974).
- 16) C. O. Bennett, *Catal. Rev. Eng. Sci.*, **12**, 105 (1976).
- 17) M. Kobayashi, *Chem. Eng. Sci.*, **37**, 393 (1982).
- 18) C. N. Satterfield, "Mass Transfer in Heterogeneous Catalysis", MIT Press, (1970).
- 19) J. O., Hirschfelder, C. F. Curtiss and R. B. Bird, "Molecular Theory of gases and Liquids", Wiley, New York, (1954).
- 20) S. L. Peluso, Ph. D. Thesis, Brown University, (1980).

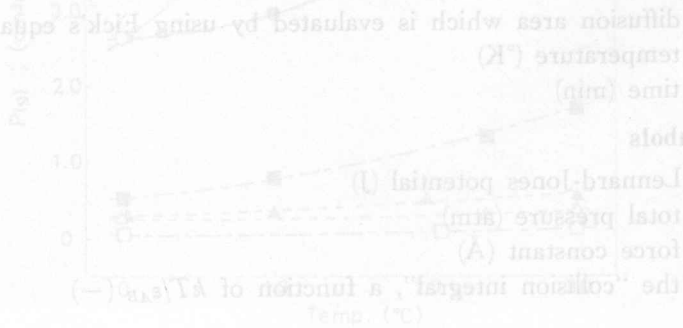


Fig. 14. The comparison of P_{O_2} of N_2 and O_2 to membrane on Ag-N-417 supported membrane as a function of Temperature.

□ : N_2 ○ : O_2 ▲ : Ag-N-417